Lab on a Chip

PAPER

View Article Online
View Journal

Cite this: DOI: 10.1039/d0lc01112f

Patterning of interconnected human brain spheroids†

Jae Jung Kim,‡[abc] Mehdi Jorfi,‡[ad] Rudolph E. Tanzi,[d] Doo Yeon Kim,[d] Patrick S. Doyle [b] and Daniel Irimia *[ac]

Received 3rd November 2020,
Accepted 1st July 2021

DOI: 10.1039/d0lc01112f

rsc.li/loc

Brain spheroids are emerging as valuable *in vitro* models that are accelerating the pace of research in various diseases. For Alzheimer's disease (AD) research, these models are enhanced using genetically engineered human neural progenitor cells and novel cell culture methods. However, despite these advances, it remains challenging to study the progression of AD *in vitro* as well as the propagation of pathogenic amyloid-β (Aβ) and tau tangles between diseased and healthy neurons using the brain spheroids model. To address this need, we designed a microfluidic system of connected microwells for arranging two types of brain spheroids in complex patterns and enabling the formation of thick bundles of neurites between the brain spheroids and the accumulation of pathogenic Aβ within the spheroids.

Introduction

Brain spheroids are promising cell culture platforms for the study of human neurological disorders. Three-dimensional (3D) brain spheroids mimic several aspects of tissue organization, are relatively easy to manipulate compared to other 3D cellular brain models, and closely recapitulate the tangled connectivity of the brain.[1–3] Empowered by the genetic engineering of human neural progenitor cells, brain spheroids recapitulate critical pathological hallmarks of Alzheimer's disease (AD).[4,5] Stem-cell-derived brain spheroids are also helpful models by recapitulating the arrangement and multiple cell types of the human brain during AD pathology.[6,7] Moreover, in combination with microfluidic methods designed to reduce the spheroid heterogeneity in size, neural progenitor cells and human-induced pluripotent stem cells (hiPSCs) have been recently used to screen various compounds to slow the progression of AD.[8] However, to reach the full potential of the brain spheroids as versatile, *in vitro* models of AD, the brain spheroids must allow the study of the propagation of pathogenic amyloid-β (Aβ) species and the monitoring of the progressive disruption of the neural networks. Towards these goals, new engineered tools to handle brain spheroids are necessary.

Arranging different types of cellular spheroids in close proximity has been tested as a method to study heterogeneous interactions between diseased and healthy neurons. For example, a neurospheroid network assembled in microwells *in vitro* was transferred onto the cortical surface of a brain and extended axons into the host cortical tissue. However, this approach has poor control of the heterogeneous interaction that could form and is limited in precision due to alignment issues.[9] A template-based centrifugation transfer method allowed the formation of vast arrays of spheroid doublets. However, the inter-space between spheroids cannot be controlled and cannot be visualized in detail.[10] When cells are isolated from the primary rat cortex, they have to be maintained in culture for at least two weeks before they start forming connections.[11–13] Although brain spheroids have been shown to be extremely useful for biological applications, no study has demonstrated high-throughput patterning of brain spheroids and robust neural connections between adjacent spheroids in long-term cell cultures.

Here we report a template-based approach to generate robust patterns of brain spheroids. As a proof of concept, we tested this approach for emulating AD pathology in a dish using brain spheroids derived from genetically engineered neural progenitor cells. We demonstrate that we could accomplish high-throughput, large-scale patterning, and inter-space connections (thick bundles) between brain spheroids.

[a] Center for Engineering in Medicine, Department of Surgery, Massachusetts General Hospital, Harvard Medical School, Charlestown, Massachusetts, USA. E-mail: daniel_irimia@hms.harvard.edu
[b] Department of Chemical Engineering, Massachusetts Institute of Technology, Cambridge, Massachusetts, USA
[c] Shriners Hospital for Children, Boston, Massachusetts, USA
[d] Genetics and Aging Research Unit, McCance Center for Brain Health, Mass General Institute for Neurodegenerative Disease, Department of Neurology, Massachusetts General Hospital, Harvard Medical School, Charlestown, Massachusetts, USA

† Electronic supplementary information (ESI) available. See DOI: 10.1039/d0lc01112f

‡ These authors contributed equally.

Methods

Fabrication of microwell arrays for sequence-specific patterning

Polydimethylsiloxane (PDMS) microwell array was molded by a fluorinated PDMS (Sylgard 184, Dow Corning) and bonded to a glass-bottom dish. PDMS base was mixed with its curing agent in a 10 : 1 ratio and cured on a top of SU-8 (Microchem) master, which was prepared by standard photolithography. Cured PDMS was cut and punched to make two holes. The punched PDMS mold was bonded to the flat PDMS block (10 : 1 mixing ratio) by using plasma treatment. A thick glass slide was placed at the bottom of the flat PDMS block to ensure flatness. Ethanol and 2% trichloro(1*H*,1*H*,2*H*,2*H*-perfluorooctyl)silane (Sigma Aldrich) were vigorously mixed by vortexing. After oxygen plasma treating, the assembled mold was filled with the ethanol–silane mixture. After 7 minutes, the mold was gently washed with ethanol and compressed air twice. The mold was baked at 80 °C for 20 minutes and washed with ethanol and water repeatedly. The mold was baked at 80 °C again until fully dried. Degassed PDMS, mixed at a 10 : 2 ratio, was placed on top of two holes after cooling the device at room temperature. The entire mold was placed in a vacuum desiccator, and the vacuum was applied to remove the trapped air. After turning off the vacuum pump, the vacuum was maintained until air bubbles were removed from the PDMS liquid on top of the mold. As the vacuum was removed, liquid PDMS was filling the mold by the pressure difference. To completely remove the air, the degassing process was repeated several times. The entire mold was cured in a 65 °C oven overnight, and the cured membrane was detached from the mold. The two PDMS sprues formed through the inlet holes of the mold are cut from the membrane with a sharp blade. The PDMS membrane is then flipped and transferred on top of a flat PDMS piece for easier handling. The PDMS membrane was bonded to a glass-bottom dish after oxygen plasma treatment, and the flat PDMS is removed. The height of channels and wells in the rectangular and checkerboard patterns were 247 and 617 μm, respectively. For the brain-like patterns, the height of the wells and channels were 806 and 446 μm, respectively.

Fabrication of patterned blocking layer

The blocking layer was fabricated from Norland Optical Adhesive 81 (NOA81, Norland Products) using a PDMS mold. The PDMS mold was assembled with a punched PDMS block on top of the thick glass slide. A drop of NOA81 was placed on top of the hole, and NOA81 filled the mold by using a vacuum, as discussed above. After ultraviolet (UV) curing, NOA81 blocking layer was detached from the mold. The block layer was placed on the PDMS microwell arrays while aligning them on top of the microscope stage.

Cell culture

We employed the immortalized human neural progenitor cell line ReNcell VM human neural stem cells (ReN) to make the brain spheroids. Human recombinant epidermal growth factor (EGF) stock solution (20 μg ml^{-1}) was prepared by filtering 10 mM acetic acid through a 0.2 μm membrane, and then 2.0 ml of the filtered acetic acid was added to 2.0 mg of lyophilized EGF (Sigma-Aldrich; 1 mg ml^{-1}) and mixed thoroughly. A final concentration of 20 μg ml^{-1} was made by further diluting with 0.2 μm filtered 0.1% (wt/vol) bovine serum albumin (BSA) solution. The human recombinant basic fibroblast growth factor (bFGF) stock solution (25 μg ml^{-1}) was prepared by filtering 10 mM Tris (pH 7.6) through a 0.2 μm membrane. Then 2.0 ml of the filtered Tris was added to 50 μg of lyophilized bFGF (Stemgent), mixed thoroughly, to make 0.2 ml aliquots. EGF and bFGF aliquots were stored at −80 °C for further use. ReN cell proliferation medium is composed of 484.5 ml DMEM/F12 medium (Gibco/Life Technologies), 0.5 ml heparin (STEMCELL Technologies), 10 ml B27 (Gibco/Life Technologies), 5.0 ml 100× penicillin/streptomycin (Lonza), 0.5 ml amphotericin B (Lonza), 0.5 ml EGF (20 μg ml^{-1}, Sigma-Aldrich), 0.4 ml bFGF (25 μg ml^{-1}, Stemgent). ReN cell differentiation medium is composed of 484.5 ml DMEM/F12 medium (Gibco/Life Technologies), 0.5 ml of heparin (STEMCELL Technologies), 10 ml of B27 (Gibco/Life Technologies), 5.0 ml 100× penicillin/streptomycin (Lonza), and 0.5 ml amphotericin B (Lonza). Matrigel-coated vented T75 cell culture flasks were prepared by adding 10 ml of Matrigel : DMEM-F12 medium (1 : 100 dilution) to the bottom of each vented T75 flask, shake gently to cover the surface, and incubated at 37 °C for 4 hours before cell culture.

Generation of brain spheroids from stem cells

Immortalized human neural progenitor cell line ReNcell VM (ReN) were transfected with internal ribosome entry site (IRES)-mediated polycistronic lentiviral vectors containing FAD-related genes encoding human amyloid precursor protein (APP) with both the K670N/M671L (Swedish) and V717I (London) mutations (APPSL), presenilin 1 (PSEN1) with the Δ*E*9 mutation (PSEN1(Δ*E*9)) with both GFP and mCherry as reporters for viral infections according to previous report.[4] To generate brain spheroids of uniform size, we employed a microfabricated PDMS device with well-arrays and a protocol, as previously described in detail.[8] Several microwell arrays of 30 × 30 microwells with different diameters (*D*) and height (*H*) were fabricated: 100 μm (*D*) × ~100 μm (*H*), 200 μm (*D*) × ~200 μm (*H*), 400 μm (*D*) × ~400 μm (*H*), 600 μm (*D*) × ~600 μm (*H*). The microwell arrays were fabricated using standard soft photolithography techniques. First, a master for preparing the PDMS array was microfabricated with SU-8100 photoresist (MicroChem Co.) on a silicon wafer. A layer (100–600 μm thick) of SU-8100 was patterned by photolithography using a photomask. Then, the PDMS array was molded by casting the liquid prepolymer composed of a mixture of 10 : 1

silicone elastomer and a curing agent (Sylgard 184). The mixture was cured at 75 °C for four hours, and the PDMS mold was peeled from the silicon wafer. The molded PDMS block was moved to 6 well plates, oxygen-plasma treated and immediately used for culturing ReN cells and generating brain spheroids at 37 °C and 5% CO_2 incubation.

The preparation of ReN cells is as follows: once ReN cells have reached 90–100% confluency in a standard T75 culture flask, the medium was aspirated, and cells dissociated. ReN cells were re-suspended with 600 µl volume of proliferation medium to achieve an appropriate final concentration. 200 µl of the cell suspension was added to the microwell array. After 20 minutes at 37 °C and 5% CO_2 atmosphere, 2.0 ml of proliferation medium was added against the wall of each well. The medium was aspirated to remove floating cells from the wells, and fresh 2 ml of proliferation medium was added to each well. The arrays were incubated at 37 °C and 5% CO_2 atmosphere. The proliferation medium was changed after 24 hours, and the arrays were incubated at 37 °C and 5% CO_2 for another 24 hours to generate fully formed brain spheroids. To remove human brain spheroids from the arrays after 48 hours, the arrays were placed in a new 6 well plate tilted at 45°, and the proliferation medium was sprayed over the array using a 1.0 ml tip. Repeat this step three times to extract all spheroids from the arrays. The brain spheroids were transferred to a 15 ml conical tube containing 2 ml proliferation medium to remove floating cell debris. The supernatant was aspirated, and fresh proliferation medium was added gently after two minutes, which allowed the spheroids to settle down the conical tube. This process was repeated two more times to make sure that the brain spheroids are free of cell debris. The final spheroids were re-suspended with 1.0 ml of proliferation medium and used for assembly. To optimize the brain spheroids formation *versus* cell density, brain spheroids were cultured for 48 hours and then imaged using an inverted Nikon Eclipse Ti microscope (Nikon Instruments). Quantitative analysis of the spheroids diameter was performed using Fiji (ImageJ) software.

Patterning of human brain spheroids

PDMS arrays were soaked with 70% ethanol for three hours at room temperature and then washed with sterile deionized water three times. Then water was aspirated, and the arrays were placed under vacuum overnight. Following that, the arrays were removed from desiccators, and 2–3 ml of expansion medium was added directly to the devices. Using media in a dish, 1 ml of media was removed and added until the majority of bubbles were removed. Then, all media was removed, and 2 ml of fresh proliferation media was added to the device. The arrays were placed in a desiccator under vacuum for another 30 min. The vacuum was released gently over 2 min, and the arrays were placed under the biosafety hood at room temperature for another 1 hour. The microwells were then checked under a microscope for any bubbles, and the devices moved to incubators at 37 °C and 5% CO_2 atmosphere. 1 hour before brain spheroids assembly, the arrays were coated with Matrigel and proliferation medium (1 : 100 dilution) by adding 1 ml and incubating the devices at 37 °C and 5% CO_2.

To assemble brain spheroids, first, the media was aspirated, and AD ReN spheroids were added on top of the array. The petri dish was shacked very gently to ensure the spheroids get into the microwells. The process was monitored under a microscope every a few minutes to ensure the assembly of all the microwells. After full assembly, the arrays were checked under a microscope, and devices were

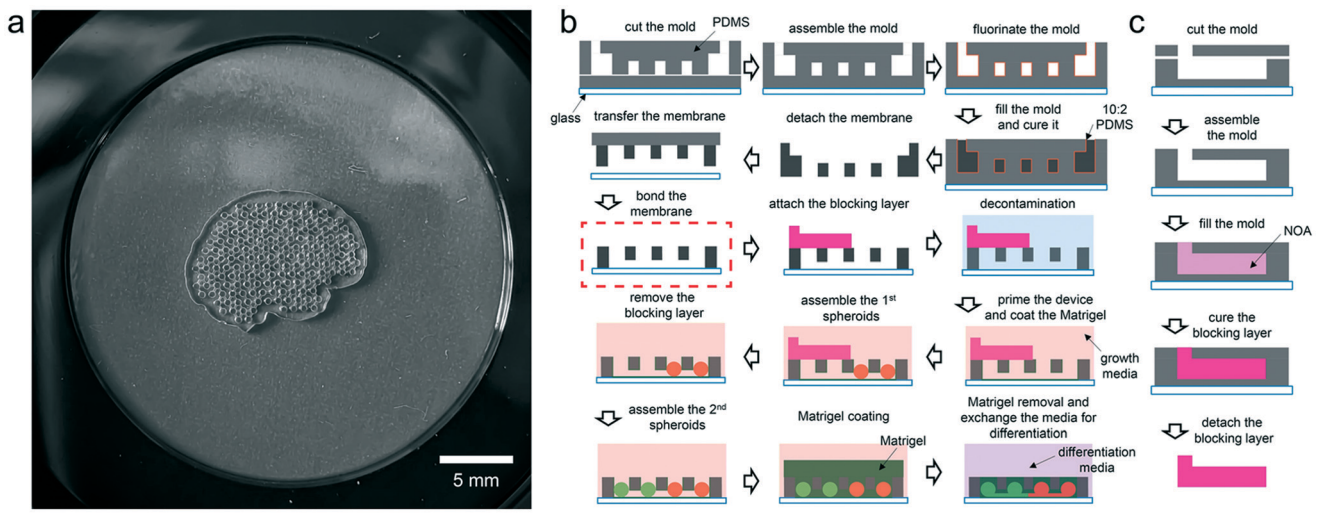

Fig. 1 Microfabrication of connected microwell arrays and assembly protocol. (a) Interconnected microwell systems (scale bar = 5 mm). (b) The construction of the microwell arrays involves fabrication of a membrane with wells and channels, the bonding of the membrane to glass, the addition of a blocking layer to direct the assembly of brain spheroids into specific patterns, and the addition of the Matrigel layer for the long-term culture of the brain spheroids. (c) Schematics show the steps for fabricating the blocking layer inside an elastomeric mold.

washed with 3–4 ml of proliferation media until all remaining unassembled spheroids have been removed from the dish. To assemble the control ReN spheroids, the blocking layer was removed, and the same steps were repeated to assemble another cell line (control). Specificity was checked under a microscope, and any unspecific assembly was removed with gel pipette tips. The arrays were incubated at 37 °C and 5% CO_2 atmosphere. After 24 hours, the entire proliferation medium was aspirated, and 100 μl of 1 : 5 Matrigel and differentiation medium (for ReN-derived spheroids) was added to each well to cover the whole surface area. The arrays were incubated at 37 °C for 2 hours to allow Matrigel to solidify. Excess Matrigel from the surface of the brain spheroids array was then removed by gently scraping using a gel loading tip that was tilted at 90° across the surface of the PDMS array. The media was replaced with 2 ml fresh pre-warmed differentiation medium. The cell culture was maintained for up to 6 weeks, changing half of the differentiation media every five days. After 4–6 weeks of differentiation, brain spheroids were rinsed with phosphate-buffered saline and fixed with 4% paraformaldehyde overnight at 4 °C and then washed three times with D-PBS. The fixed brain spheroids were imaged using an inverted Nikon Eclipse Ti microscope (Nikon Instruments).

Immunofluorescence staining

Brain spheroids were cultured up to 4–6 weeks in differentiation medium followed by rinsing in phosphate-buffered saline and fixation in 4% paraformaldehyde for overnight at room temperature and then washed three times with 1× Tris buffered saline with Tween 20 (TBS-T). The spheroids were immersed overnight at 4 °C in a blocking solution. Blocking/dilution solution for immunostaining was prepared by adding 2.5 g of BSA (Sigma-Aldrich), 5.63 g of glycine, and 0.25 g of gelatin in 200 mL of TBS-T and heated at 55 °C for ~10 min to allow the gelatin to dissolve. 10 mL of donkey serum (Sigma-Aldrich) and TBS-T was added to

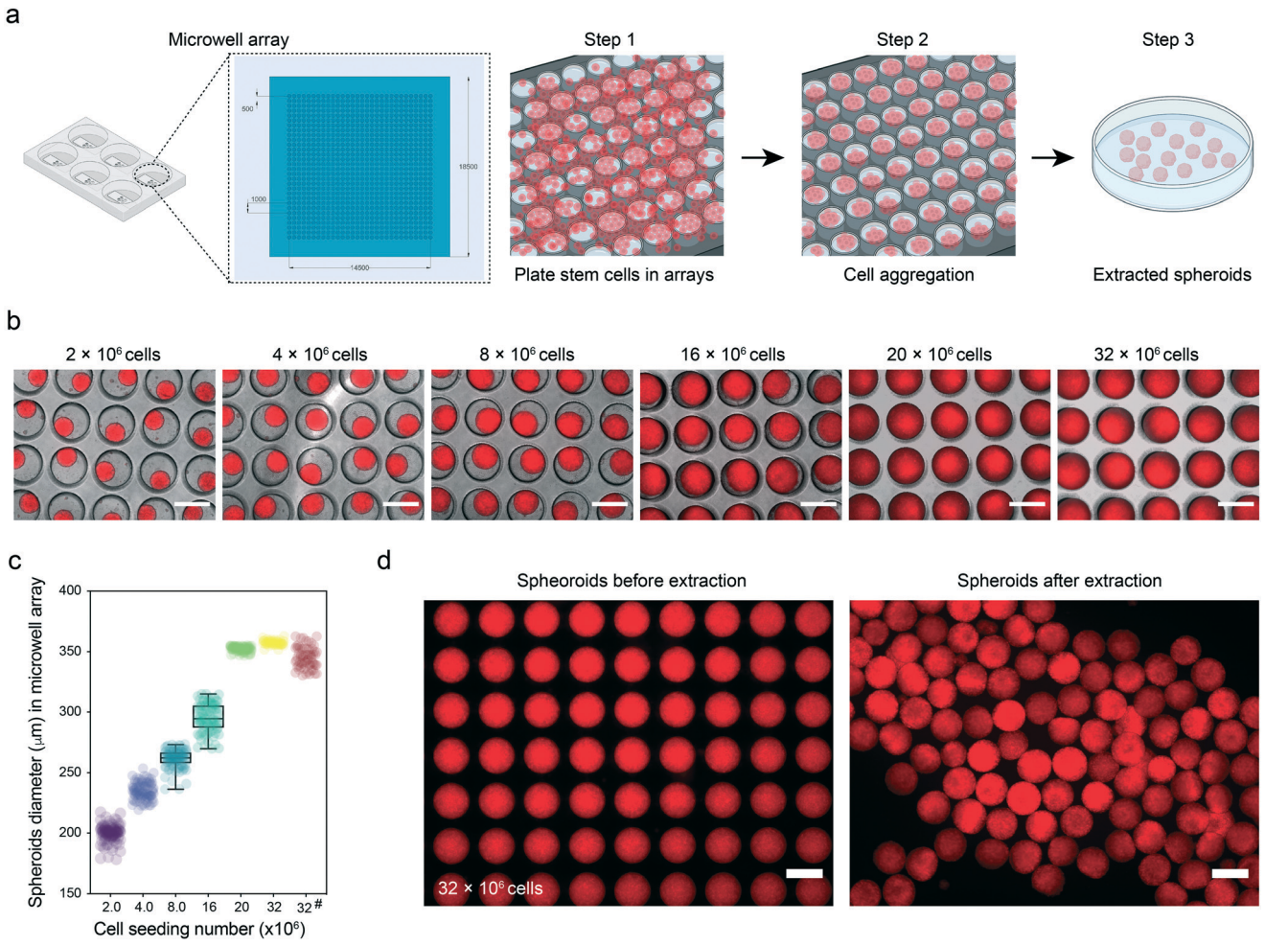

Fig. 2 Generation and recovery of uniformly-sized brain spheroids in high-throughput arrays. (a) Schematic depict the three steps towards generating uniformly-sized brain spheroids and their collection for use in the interconnected microwell arrays. (b) Brain spheroids formed in the 400 μm well after 48 hours culture at various cell seeding numbers (scale bar = 400 μm). (c) The plot shows the formation of brain spheroids in the 400 μm array *versus* cell seeding numbers (means ± SEM, $N > 100$ spheroids for each condition). #depicts spheroids after extraction. (d) Confocal images of plated and harvested homogenously sized brain spheroids generated in 400 μm arrays at 48 hours post culture (scale bar = 400 μm).

make the final volume of 250 ml. The blocking/dilution solution was then filtered with a 0.4 μm filter unit (Gibco) and stored at 4 °C. The blocking step was followed by permeabilization with 0.1% Triton X-100 for 45–60 min at room temperature. The spheroids were washed three times with 1× TBS-T and then incubated with 1 : 400 chicken anti-MAP2 (AB5543, EMD Millipore) and 1 : 200 rabbit anti-Aβ42 (cell signaling) in blocking solution at 4 °C overnight followed by species-specific secondary antibodies at 4 °C overnight in the dark. The brain spheroids were then imaged using an inverted Nikon Eclipse Ti microscope (Nikon Instruments) and processed using Fiji (ImageJ) software.

Quantification of the connection rate

The connection rate is defined as the number of connections through the bottom channel between two adjacent spheroids per the total number of channels between spheroid-loaded wells. We counted all the connections through the channels, regardless of their thickness. The connection rate was quantified for each brain spheroid-pair-type: control–control, control–AD, and AD–AD.

Quantitative measurement of bundles

Brain spheroids at 3 week differentiation were fixed in 4% paraformaldehyde and imaged using an inverted Nikon Eclipse Ti microscope (Nikon Instruments). The images were processed with NIS software, which allowed projections of the data in the *Z* direction and 3D visualization. The images were resliced, and 3D visualization of bundles was constructed. The thickness of spheroid–spheroid bundles was measured using 3D constructed images and reported as means ± SEM for N = 17–20 for 1 : 100 Matrigel coating and N = 3–10 for no Matrigel coating or 1 : 500. Statistical analysis was performed using two-way ANOVA and corrected for multiple comparisons using the Tukey test.

Quantitative measurement of changes in amyloid-β

Aβ38, 40, and 42 levels were measured by MesoScale Discovery (MSD, Rockville, MD) 96-well Mouse Pro-inflammatory V-PLEX assay as outlined in the manufacturer's protocol. Briefly, 150 μl of diluent was added to the plate coated with an array of Aβ capture antibodies and incubated at room temperature with shaking for one hour, followed by washing with wash buffer (provided in the kit). A volume of 25 μl of the detection antibody solution plus 25 μl of prepared samples were added and incubated for two hours with vigorous shaking at room temperature. The plate was washed with wash buffer before adding 150 μl of 2× read buffer T and immediately read on a Meso QuickPlex SQ 120.

Statistical analysis

All statistical analyses were performed using GraphPad Prism 9. Quantitative analysis of the brain spheroids diameter was performed using Fiji (ImageJ) software.

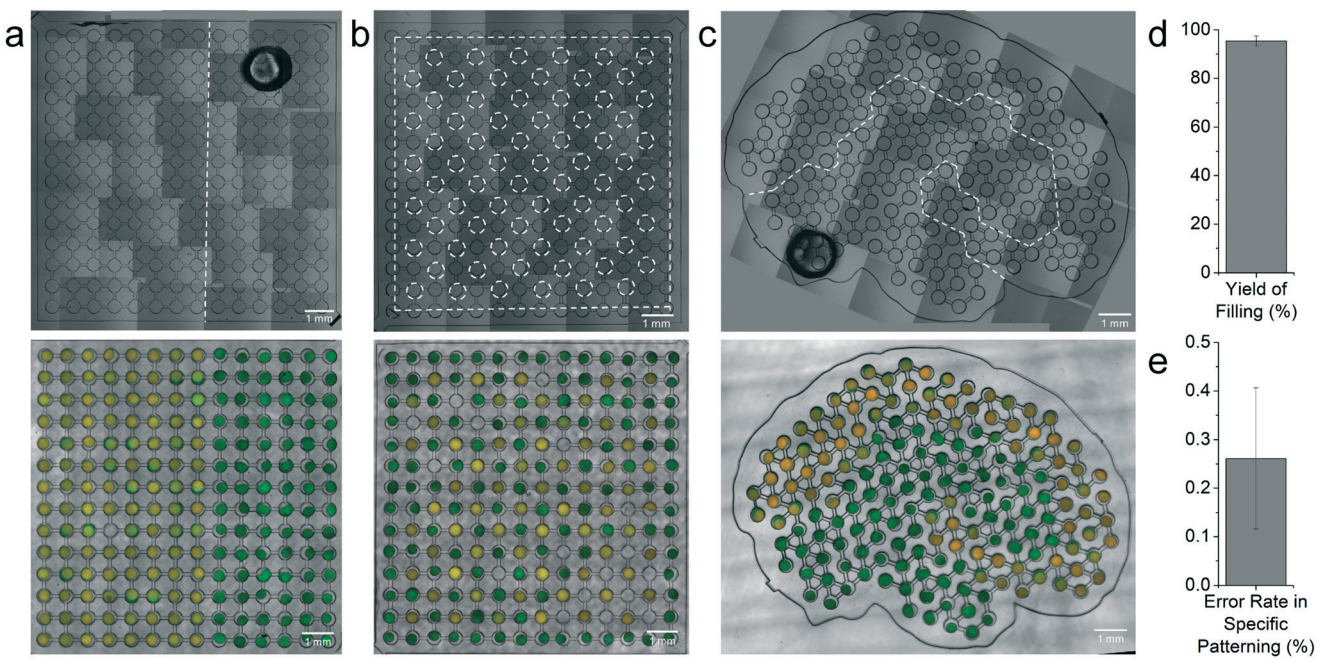

Fig. 3 Geometry fine-tuned microwell arrays for various patterns of brain spheroids. (a) Rectangular pattern. (b) Checkerboard pattern. (c) Brain-like pattern. The top row shows the bright-field images of the microwell arrays. The bottom row represents the merged channel images of specifically arranged brain spheroids right after the patterning. Yellow and green spheroids represent the AD model (ReN#H10) and control spheroids (ReN#G10), respectively. The white dotted line represents the boundary of the blocking layer. Scale bars indicate 1 mm. (d) The bar graph shows the yield of filling (mean ± SEM, N = 18). (e) The bar graph shows the error rate in specific patterning (mean ± SEM, N = 18).

Results and discussion

We fabricated PDMS membranes with interconnected arrays of microwells using a vacuum-assisted molding method (Fig. 1). The mold was fluorinated to ensure easy detachment from the membrane. For the membrane fabrication, we injected PDMS mixed at 10 : 2 ratio rather than the recommended 10 : 1 ratio to facilitate the flow of PDMS into the mold and ensure fast curing in the small confinement. The cured membrane was bonded to the glass, forming conduits between individual wells. These conduits were designed to facilitate the visualization of the spheroid–spheroid connections. Locating the conduits between spheroids at the bottom of the arrays is essential to ensure high-quality imaging of the thick bundles between interconnected spheroids and to protect these connections during media changes.

We fabricated a blocking layer using a vacuum-assisted molding method and used it to pattern different cellular spheroids within the same array (Fig. 1b). The blocking layer was placed on top of the microwell arrays to selectively cover some of the wells of the array and provide a mechanical barrier for directing the brain spheroids from a suspension to specific wells in the array. The blocking layer was aligned on the microwells using a microscope and easily can be removed during the assembly process to arrange different types of spheroids. The design of the blocking array shape is very versatile, which enables the technique to incorporate different patterns.

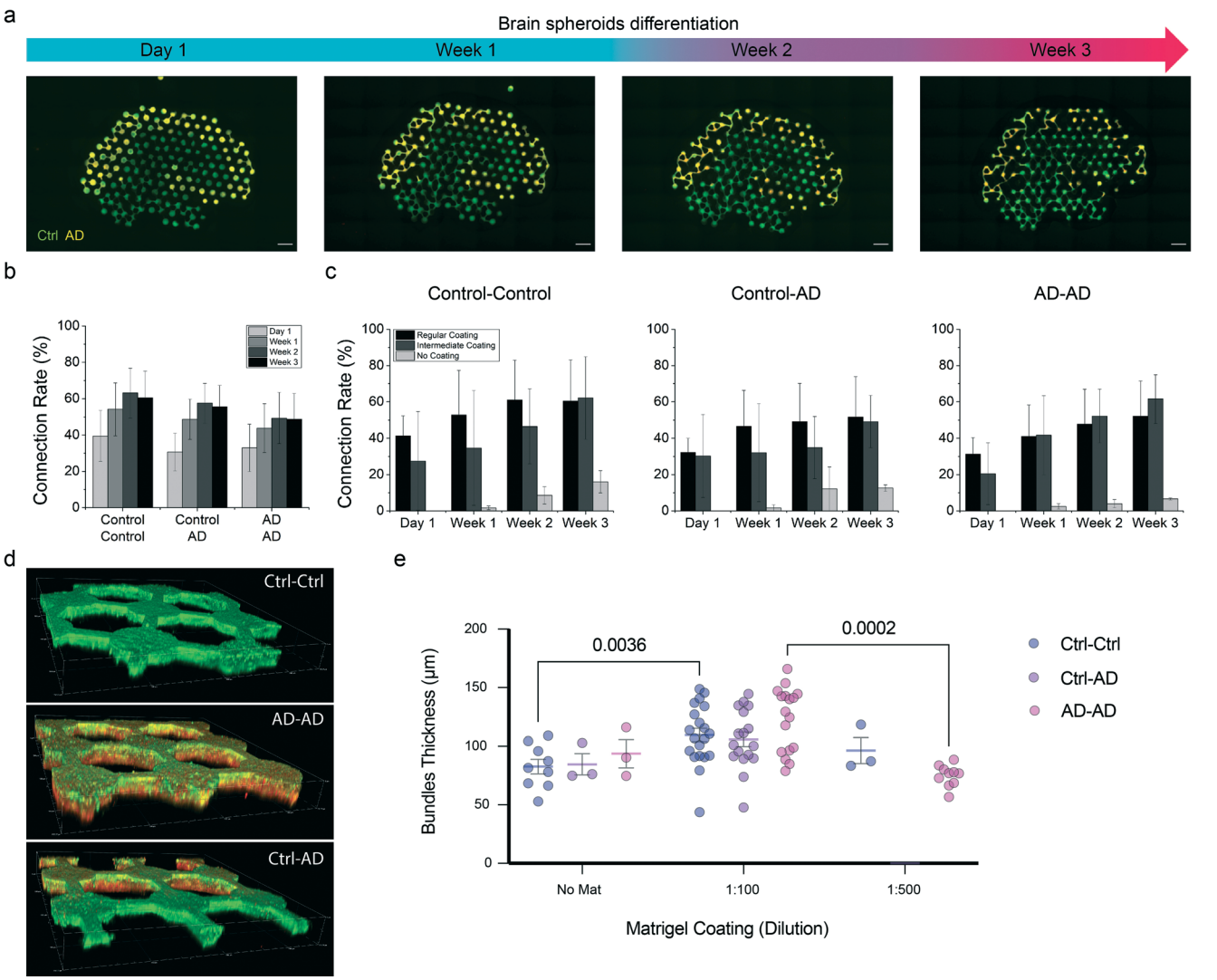

Fig. 4 Brain spheroid differentiation and inter-spheroid connections. (a) Interconnected AD and control brain spheroids are arranged on a pattern replicating the AD human brain (scale bars = 1 mm). (b) The graphs show the connection rates between distinct types of adjacent spheroid pairs (means ± SEM, N = 8 for control–control and AD-AD, or 11 for control-AD). Most connections form during the first day after the spheroid assembly. (c) The graphs display the connection rates between adjacent brain spheroids depending on Matrigel coating conditions (means ± SEM, N = 3 or 4). (d) Representative z-stack 3D construction of spheroid–spheroid bundles at 3 week differentiation. (e) The graph represents the quantification of spheroid–spheroid bundles thickness in the array after 3 week differentiation (means ± SEM, N = 17–20 for 1 : 100 Matrigel coating and N = 3–10 for no Matrigel coating or 1 : 500).

To pattern the brain spheroids, a suspension of uniformly sized brain spheroids was placed on top of the microwells. These stem-cell-derived brain spheroids are generated from genetically engineered ReNcell VM human neural stem (ReN) cells, as described before.[4,5] After gently shaking the device for 5–10 seconds, the brain spheroids settled into the accessible microwells within 10–30 seconds. Due to the large size of spheroids, gravity alone is sufficient for the fast assembly of the brain spheroids in wells. In addition, such a small driving force for assembly is desired to avoid the spheroid deformation and not affect their phenotype. By repeating the brain spheroid loading process several times, all accessible wells in the arrays were filled in less than 10 minutes. After removing all redundant brain spheroids, the blocking layer was removed, and the second type of spheroids was loaded in the remaining empty wells using a similar protocol. We found that, sometimes, more than one spheroid enters one microwell, likely due to a brain spheroid having a smaller diameter compared to the height of the microwells. To compensate for the disruption of the patterns when two brain spheroids entered the same well, we arranged the AD spheroids first. The control spheroids were loaded in a second step, and whenever they settled in a well already occupied by an AD brain spheroid, the resulting brain spheroid had AD features, matching the original design of the patterns.

Considering the importance of the precise control of brain spheroid diameter for the correct patterning, we optimized a protocol previously described for the generation of brain spheroids of uniform size.[8] Briefly, PDMS arrays of 900 microwells with different sizes were fabricated using standard soft photolithography and utilized as a platform to generate high-throughput uniformly sized spheroids for patterning. We determined the effect of changing the diameter of microwells (from 100 to 600 μm) and cell seeding numbers (from 2 to 32 × 10^6 cells/array) on the distribution of brain spheroid diameter (Fig. 2). We found that a 400 μm diameter template provides the most homogenously sized brain spheroids after formation (357.2 ± 1.9 μm) and recovery (345.5 ± 8.7 μm) using 32 × 10^6 cells/array. The optimal well size for uniformly sized brain spheroids is similar to the one reported before for various cell types,[8,14,15] and likely reflecting a balance between optimal access of nutrients and oxygen to the center of the spheroids and sufficient support between adjacent cells for a stable spheroid. The small but inevitable heterogeneity in spheroid size does not limit our technology because it does not rely on the characteristics of spheroids (*i.e.*, size and modulus) for the specific arrangement. Moreover, the intrinsic low adherence characteristic of PDMS facilitates non-adhered cellular spheroids formation and easy recovery of the spheroids from the arrays after they are fully formed.

To evaluate the performance of the brain spheroid patterning, we defined the error rate in specific patterning as the number of microwells falsely filled with AD spheroids per the total number of microwells filled with AD spheroids. We assembled brain spheroids into the rectangular, checkerboard, and brain-like designs (Fig. 3a–c). The filling yield was as high as 95.4 ± 2.1% (Fig. 3d, N = 18). The corresponding error in specificity of patterning was 0.26 ± 0.15% (Fig. 3e, N = 18).

We quantified the rate of new connections formed between adjacent spheroids on the three templates when coated with 100× diluted Matrigel (Fig. 4a and ESI† Fig. S1). Between days 0 and 1, the number of connections increased by 39.5 ± 14.0% for control–control, 30.7 ± 10.4% for control–AD, and 33.0 ± 13.1% for AD–AD spheroid pairs (Fig. 4b). Between day 1 and week 2, the rate of formation of new connection was 1.8 ± 1.9% per day for control–control, 2.1 ± 1.6% per day for control–AD, and 1.3 ± 2.0% per day for AD–AD pairs. Between weeks 2 and 3, the rate of new connection formation decreased to −0.4 ± 2.1% per day for control–control, −0.3 ± 1.7% per day for control–AD, and −0.1 ± 2.0% per day for AD–AD pairs. We also noticed that at 3 week-differentiation, only 82.0 ± 10.7% (N = 3) of the microwells originally filed were still filled by spheroids. The loss of spheroids during long-term cultures was associated with the culture media exchanges every four days.

Using the rectangular pattern, we quantified the connection rate and bundle thickness between spheroids depending on the Matrigel coating condition (Fig. 4c–e). The connection rate was higher in the presence of Matrigel at 100× and 500× dilutions than in the absence of Matrigel coating for all brain spheroid pairs: control–control, AD–control, and AD–AD (Fig. 4c). The differences were not statistically significant because of the high variation in connection rates in the presence of Matrigel coating. The variation may be explained by the batch-to-batch variation between spheroids in different experiments and the limitations of access to the bottom channels filled by the Matrigel. We also measured the thickness of bundles between adjacent spheroids after 3 week of differentiation (Fig. 4d and e). At 3 week differentiation, bundle thickness was 106.7 ± 28, 111.7 ± 22, and 123.1 ± 27 μm for control–control, control–AD and AD–AD in 1 : 100 Matrigel coating, while bundle thickness was 82.7 ± 18, 84.7 ± 16, and 93.7 ± 21 μm for control–control, control–AD and AD–AD in no Matrigel coating condition (Fig. 4e). There is a significant difference in the control–control bundle thicknesses between 1 : 100 Matrigel coating and no coating (P = 0.0036). Finally, in the 1 : 500 Matrigel coating (intermediate), bundle thickness was 96.4 ± 19, and 75 ± 9 μm for control–control, and AD–AD, respectively. We found a significant difference between AD–AD bundle thicknesses between 1 : 100 and 1 : 500 Matrigel coating (P = 0.0002). Overall, we found that the bundle thickness between control–control and AD–AD were higher in the 1 : 100 Matrigel coating condition compared to no Matrigel coating or 1 : 500 coating (intermediate).

To recapitulate AD pathology *in vitro* and assess our patterned spheroids method for long term culture, human ReN neural progenitor cells were developed according to our previous reports[4,5] to express FAD mutations overexpressing human amyloid precursor protein (APP) and presenilin 1

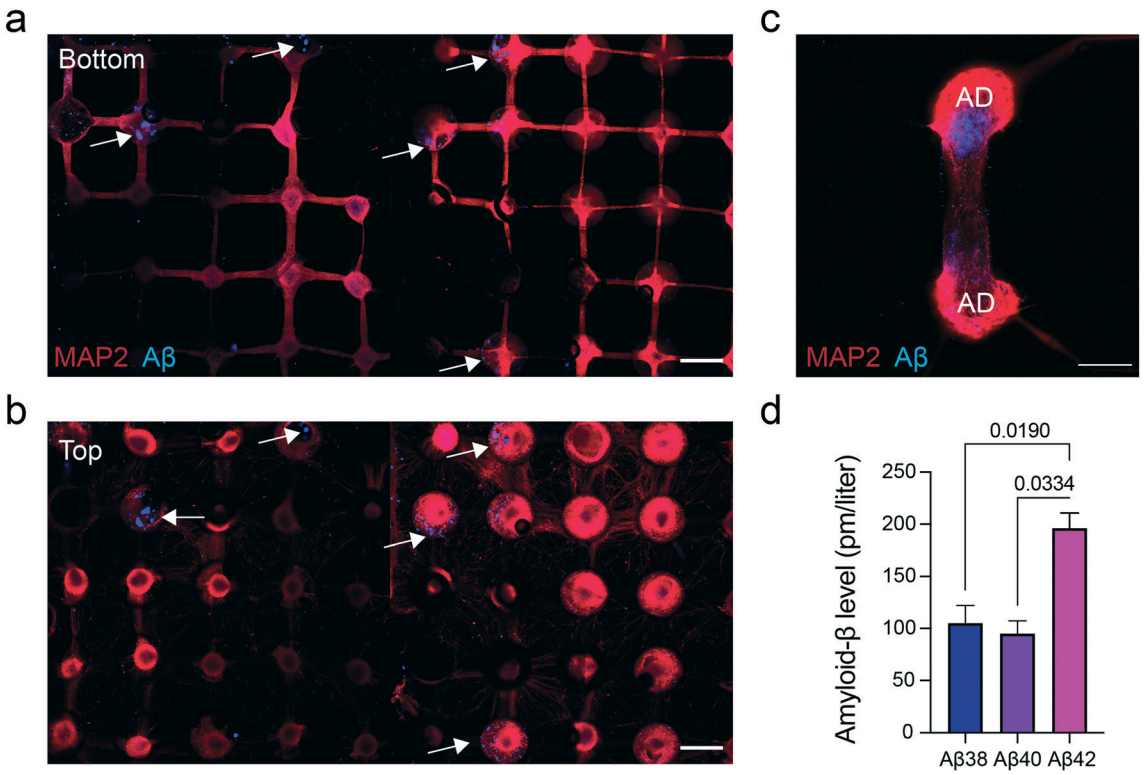

Fig. 5 Brain spheroid differentiation and AD pathology recapitulation. (a–c) Representative confocal images show expression of neuronal marker (MAP-2, microtubule-associated protein 2; red), and Aβ42 (blue) in the brain spheroids at six-week differentiation. Images represent the top and bottom of the arrays. (d) The graph shows quantification of Aβ38, 40, and 42 in the collected media from six-week-old brain spheroids using ELISA (means ± SEM, $N = 4$).

(PSEN1).[16] Control (ReN#G10) and FAD-derived (ReN#H10) brain spheroids were patterned and cultured in the array platform with Matrigel and differentiated over the course of 6 weeks. At 1 week after the start of differentiation in the array, we observed thick neural bundles and processes extend to adjacent human brain spheroids through interconnected channels and from the top of the arrays, both in control (ReN#G10) and in AD (ReN#H10) as well (Fig. 4a), suggesting the formation of the neuronal network. This is in line with our previous observation, where we found that brain spheroids with AD mutations generate neural connections as early as day 7 after differentiation.[8] As a proof of concept to detect and analyze AD markers in FAD-derived human brain spheroids, the spheroids were fixed with 4% PFA after 6 week differentiation and stained for Aβ and microtubule-associated protein 2 (MAP-2). Using immunofluorescence staining, we observed expressed neuronal marker, MAP-2 (Fig. 5a–c), and accumulated Aβ plaques in the FAD brain spheroids (ReN#H10) as well as in the thick bundles connecting the adjacent human spheroids in the arrays (Fig. 5a–c) Aβ levels in the cell media were also measured by Aβ ELISA kit. We detected soluble Aβ species in the culture media from the 6 week-differentiated control-AD brain spheroids co-cultured in the rectangular pattern array shown in Fig. 3a. As expected in AD pathology, we observed a higher Aβ42 level compared to Aβ38 and Aβ40 (Fig. 5d).

Conclusions

We designed a microfluidic array of connected wells for arranging two types of brain spheroids in complex patterns. We found that physical blocking using a molded blocking layer positioned at a pre-defined location can be a robust method for precision patterning of cellular spheroids in wells with high specificity. We show that thick bundles of neurites form between the brain spheroids and demonstrate the accumulation of pathogenic Aβ within the spheroids. In the future, multiple blocking layers may be useful for patterning more than two types of cellular spheroids to mimic complex tissue patterns.

Conflicts of interest

There are no conflicts to declare.

Acknowledgements

The authors acknowledge Miss Anika Marand for her help during the project. This work was supported by the National Institutes of Health (GM092804, AG061891, AG062547 and NS121078) and Cure Alzheimer's Fund. Microfabrication procedures were performed at the BioMEMS Core at the Mass General Brigham (https://researchcores.partners.org/biomem/about) and the Massachusetts Institute of Technology.

References

1 R. M. Marton and S. P. Pasca, *Cell Stem Cell*, 2016, **19**, 145–146.
2 F. Birey, J. Andersen, C. D. Makinson, S. Islam, W. Wei, N. Huber, H. C. Fan, K. R. C. Metzler, G. Panagiotakos, N. Thom, N. A. O'Rourke, L. M. Steinmetz, J. A. Bernstein, J. Hallmayer, J. R. Huguenard and S. P. Pasca, *Nature*, 2017, **545**, 54–59.
3 M. Jorfi, C. D'Avanzo, D. Y. Kim and D. Irimia, *Adv. Healthcare Mater.*, 2018, **7**, 1700723.
4 S. H. Choi, Y. H. Kim, M. Hebisch, C. Sliwinski, S. Lee, C. D'Avanzo, H. Chen, B. Hooli, C. Asselin, J. Muffat, J. B. Klee, C. Zhang, B. J. Wainger, M. Peitz, D. M. Kovacs, C. J. Woolf, S. L. Wagner, R. E. Tanzi and D. Y. Kim, *Nature*, 2014, **515**, 274–278.
5 Y. H. Kim, S. H. Choi, C. D'Avanzo, M. Hebisch, C. Sliwinski, E. Bylykbashi, K. J. Washicosky, J. B. Klee, O. Brüstle, R. E. Tanzi and D. Y. Kim, *Nat. Protoc.*, 2015, **10**, 985–1006.
6 J. K. Harrison, J. V. Joseph, I. A. M. V. Roosmalen, E. Busschers, T. Tomar, S. Conroy, E. Eggens-Meijer, N. Peñaranda Fajardo, M. M. Pore, V. Balasubramanyian, M. Wagemakers, S. Copray, W. F. A. D. Dunnen and F. A. E. Kruyt, *PLoS One*, 2015, **10**, e0145393.
7 C. D'Avanzo, C. Sliwinski, S. L. Wagner, R. E. Tanzi, D. Y. Kim and D. M. Kovacs, *FASEB J.*, 2015, **29**, 3335–3341.
8 M. Jorfi, C. D'Avanzo, R. E. Tanzi, D. Y. Kim and D. Irimia, *Sci. Rep.*, 2018, **8**, 2450.
9 M. Kato-Negishi, Y. Tsuda, H. Onoe and S. Takeuchi, *Biomaterials*, 2010, **31**, 8939–8945.
10 M. J. Susienka, B. T. Wilks and J. R. Morgan, *Biofabrication*, 2016, **8**, 045003.
11 Y. Y. Choi, B. G. Chung, D. H. Lee, A. Khademhosseini, J. H. Kim and S. H. Lee, *Biomaterials*, 2010, **31**, 4296–4303.
12 G. S. Jeong, J. Y. Chang, J. S. Park, S. A. Lee, D. Park, J. Woo, H. An, C. J. Lee and S. H. Lee, *Mol. Brain*, 2015, **8**, 17.
13 Y. T. Dingle, M. E. Boutin, A. M. Chirila, L. L. Livi, N. R. Labriola, L. M. Jakubek, J. R. Morgan, E. M. Darling, J. A. Kauer and D. Hoffman-Kim, *Tissue Eng., Part C*, 2015, **21**, 1274–1283.
14 X. Gong, C. Lin, J. Cheng, J. Su, H. Zhao, T. Liu, X. Wen and P. Zhao, *PLoS One*, 2015, **10**, e0130348.
15 G. Pettinato, X. Wen and N. Zhang, *Sci. Rep.*, 2014, **4**, 7402.
16 S. S. Kwak, K. J. Washicosky, E. Brand, D. von Maydell, J. Aronson, S. Kim, D. E. Capen, M. Cetinbas, R. Sadreyev, S. Ning, E. Bylykbashi, W. Xia, S. L. Wagner, S. H. Choi, R. E. Tanzi and D. Y. Kim, *Nat. Commun.*, 2020, **11**, 1377.